NON-DIMENSIONAL AXIAL LOAD-MOMENT INTERACTION DIAGRAMS FOR FRP STRENGTHENED MASONRY WALLS

Sonia Martínez 1, M. Dolores García2, J. Pedro Gutiérrez1
[1] *IETCC, CSIC. Eduardo Torroja Institute for Construction Science, Spain. Email: soniamdm@ietcc.csic.es*
[2] *ETSAM, UPM. Superior Technical School of Architecture of Madrid, Spain*

ABSTRACT:

Masonry is a material with poor capacity to withstand tensile loads, for this reason it results so vulnerable against destabilizing accidental loads, such as earthquakes. External FRP (fibre reinforced polymer) reinforcements can improve out-of-plane flexural capacity of masonry walls. For practical applications, we need to study the critical sections to check Ultimate Limit State is not exceeded. In this sense, non-dimensional axial load-moment interaction diagrams are a useful tool for the design/assessment of the FRP reinforcement, as well as for analyzing the incidence of the main variables on the ultimate cross sectional capacity. The diagrams included in this work have been prepared from a calculation procedure similar to that used for reinforced concrete sections but adapted to the particularities of the strengthened masonry ones. For masonry, an idealized bilinear stress-strain relationship is used. For FRP strengthening, linear elastic up to failure, the design strain for flexural applications is limited by a "bond reduction factor" taking into account some aspects, such as intermediate FRP debonding failure, that causes the FRP sheets can't reach their ultimate tensile strength although their ends were properly anchored. Non dimensional axial load-moment interaction diagrams are presented, which main parameters have been chosen to be representative of different FRP strengthening systems. These diagrams allow analyzing the predictable failure mode (due to masonry or FRP) and the improvement of flexural sectional cross capacity obtained by means of the strengthening depending on axial load level supported by the wall.

KEYWORDS

Composites, FRP, Masonry structures, Strengthening, Load-moment interaction diagrams.

INTRODUTION

Masonry is characterized for being a good material to support compressive stresses but really bad to withstand tensile ones. For this reason, unreinforced masonry walls are vulnerable to earthquake or high wind loading. On the other hand, glue FRP laminates can improve the flexural capacity of masonry elements subject to bending.
This kind of strengthening may be interesting mainly in the event of damage due to exceptional events (such as earthquakes), damage occurring with time in the life of a building (such as differential soil settlement) or in the event of an increase in live loads (Di Tomasso 2001). Several samples of this technique applied to masonry elements have been carried out, mainly in Italy (Celestini 2009).
Experimental tests have shown that FRP materials can improve significantly the out-of-plane bending capacity of masonry walls. However, most of them have been carried out in pure bending (Triantafillou 1998, Albert 1998, Velázquez-Dimas 2000, Hamilton 2001, Morbin 2002, Tan 2004, Mosallam 2007). Only some tests were tested combining bending and compression (Barbieri 2000, Galati 2003, Accardi 2007, Martínez 2013). This is an important issue because most of the masonry elements in historical buildings have a structural bearing function.
In regards of theoretical studies, there are different proposals based on reinforced concrete analytical methods (Triantafillou 1998, Albert 1998, Velázquez-Dimas 2000, Hamilton 2001 Tan 2004, Mosallam 2007). However, they present important differences regarding the constitutive law of masonry (elastic approach or a simplified rectangular stress block), the way of assessing the FRP design strain or the desirable failure mode that it must be looked for. An U.L.S. method to design and check FRP strengthened masonry sections subject to bending and compression is proposed, including a "bond factor" to assess the FRP design strain. Later, different axial load-moment interaction diagrams are drawn with the aid of the proposed formulation.

CALCULATING METHOD FOR ULS

A method, similar to that used for RC sections but adapted to the particularities of the strengthened masonry ones, has been proposed (Martínez, 2014). It is applicable for FRP strengthened masonry walls with properly anchored FRP ends. According to experimental studies, FRP strengthened masonry walls with anchored FRP ends subject to bending can fail due to: 1) crushing masonry, 2) FRP rupture and 3) intermediate FRP laminate debonding from masonry substrate, usually induced by intermediate flexural cracks.

DESIGN BASIS AND MATERIALS

In regard to masonry, its tensile strength is considered negligible and an idealized bilinear stress-strain relationship is used, Figure 1a. The first phase of the stress-strain diagram (elastic phase) is defined by Eq. 1, and the second one (plastic phase) by Eq. 2. The modulus of elasticity for masonry (E_m) is assessed as the product of the design compressive strength (f_{md}) by a factor (β). According to the bibliography on masonry (Hendry, 1998), this factor β could take a value from 1000 to 400, in this work a value of 750 is adopted. The value of masonry ultimate strain (ε_{mu}) is considered equal to 0.0035 as Eurocode 6.

If $0 < \varepsilon_m \leq \varepsilon_{me}$ then $\sigma = E_m \varepsilon_m$ (1)

If $\varepsilon_{me} < \varepsilon_m \leq \varepsilon_{mu}$ then $\sigma = f_{md}$ (2)

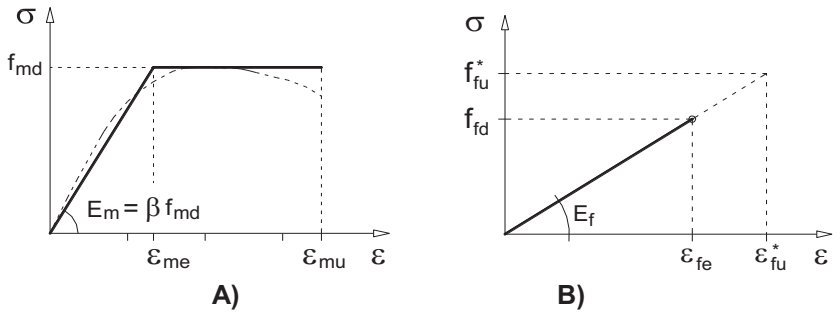

Figure 1: Stress-strain diagram for: a) masonry and b) FRP strengthening.

In regard to FRP material, it is considered linear elastic up to failure, Figure 1b. Up to the design strain value (ε_{fe}), a full composite action between composite strip and the masonry surface is assumed. The FRP thickness is considered negligible. Eqs. 3-4 allow to calculate FRP design tensile stress (f_{fd}) and strain (ε_{fe}) by means of the ultimate tensile fiber strain (ε_{fu}^*) and two factors. The "*environment reduction factor*" or C_E takes into account the effects of long-term exposure to different environments and the "*bond reduction factor*" or K limits the FRP design strain to prevent FRP debonding failure induced by intermediate cracks.

$f_{fd} = E_f \varepsilon_{fe}$ (3)

$\varepsilon_{fe} = K C_E \varepsilon_{fu}^*$ (4)

The environment factor (C_E) can be taken from ACI codes. The bond reduction factor (K), relatively similar to ACI 440.7R-10, has been fixed with the aid of a large bending test database. It has been extracted from 9 studies of the existing literature and from an own small experimental program (Martínez, 2013).

The proposed values of K are:

K=0.40 for FRP wet lay-up systems(5)

K=0.25 for CFRP pultruded laminates (6)

LIMIT STRAIN DOMAINS

The failure modes can be related to the strain distribution of the critical section, see Figure 2. It is accepted plane hypothesis of strain of the strengthened section.

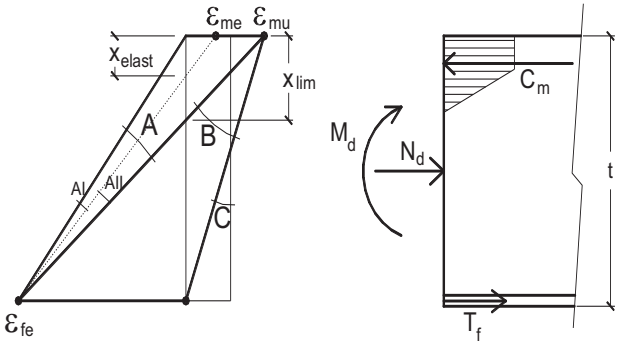

Figure 2: Strain and stress distribution

The domain or region "A" corresponds with a failure due to an excess of deformation in the FRP laminate (including debonding or rupture). The region "B" corresponds with a crushing masonry failure. The region "C", in which compression loads are predominant, it is not proper for FRP flexural strengthening. The flexural capacity of FRP strengthened wall depends on the predictable failure mode. Design equations are given below.

EQUATIONS FOR U.L.S. METHOD

It is considered a masonry wall of width "l" and thickness "t" subject to out-of-plane bending (M_d) combined with compression (N_d) and strengthened by bonding an FRP laminate of width "b_f" and thickness "t_f". The mechanical FRP reinforcement ratio (ϖ_f) can be calculated by Eq. 7. When failure is due by masonry and FRP simultaneously this ratio has been called "limit reinforcement ratio" ($\varpi_{f,\,lim}$) and can be calculated by Eq. 8. When failure is due FRP while masonry still behaves elastically, the ratio is called "elastic reinforcement ratio" ($\varpi_{f,\,elást}$) and can be calculated by Eq. 9. In both expressions, "ν" is the normalized axial load (equal to $N_d/t\ b\ f_{md}$).

$$\varpi_f = (b_f\ t_f\ f_{fd}) / (b\ t\ f_{md}) \qquad (7)$$

$$\varpi_{f,\,lim} = \left(1 - \frac{0{,}5}{\beta\ \varepsilon_{mu}}\right) \frac{1}{\left(1 + \frac{\varepsilon_{fe}}{\varepsilon_{mu}}\right)} - \nu \qquad (8)$$

$$\varpi_{f,\,elást} = \frac{0{,}5}{(1 + \beta\ \varepsilon_{fe})} - \nu \qquad (9)$$

The predictable failure mode can be determined by comparing the FRP reinforcement ratio of the strengthened wall to the "*elastic*" and "*limit*" ratios. Based on the strain compatibility principle and forces and moment equilibrium, formulation for each case can be obtained.

When $\omega_f < \omega_{f,elas}$, the failure is due to debonding or rupture of FRP while the masonry exhibits linear behaviour. The Equations 10-11 allow calculating the ratio depth of the neutral axis to masonry thickness (x/t) and the normalized ultimate moment of the strengthened section (μ).

$$0{,}5\ \beta\ \varepsilon_{fe} \left(\frac{x}{t}\right)^2 + (\omega_f + \nu)\left(\frac{x}{t}\right) - (\omega_f + \nu) = 0 \qquad (10)$$

$$\mu = 0{,}5\ \beta\ \varepsilon_{fe} \frac{\left(\frac{x}{t}\right)^2}{\left(1 - \frac{x}{t}\right)} \left(0{,}5 - \frac{1}{3}\frac{x}{t}\right) + 0{,}5\ \omega_f \qquad (11)$$

When $\omega_{f,elas} < \omega_f < \omega_{f,lim}$, the failure is due to debonding or rupture of FRP while the masonry exhibits nonlinear behaviour and the Equations are 12-14.

$$\left(\frac{x}{t}\right) = (\nu + \omega_f + 0{,}5\ \frac{1}{\beta\varepsilon_{fe}}) / (1 + \ 0{,}5\frac{1}{\beta\varepsilon_{fe}}) \qquad (12)$$

$$\mu = 0{,}5\left(\frac{x}{t} - \frac{a}{t}\right)\left(1 - \frac{x}{t} + \frac{a}{t}\right) + 0{,}5\left(\frac{a}{t}\right)\left(0{,}5 - \frac{x}{t} + \frac{2}{3}\frac{a}{t}\right) + 0{,}5\ \omega_f \qquad (13)$$

$$\text{con } \left(\frac{a}{t}\right) = \frac{\varepsilon_{me}}{\varepsilon_{fe}}\ (1 - \frac{x}{t}) \qquad (14)$$

When $\omega_f > \omega_{f,lim}$, the failure is due to crushing masonry and the Equations are 15-17.

$$(1 - 0{,}5\frac{\varepsilon_{me}}{\varepsilon_{mu}})\left(\frac{x}{t}\right)^2 + \left(\omega_f \frac{\varepsilon_{mu}}{\varepsilon_{fe}} - \nu\right)\left(\frac{x}{t}\right) - \left(\omega_f \frac{\varepsilon_{mu}}{\varepsilon_{fe}}\right) = 0 \qquad (15)$$

$$\mu = 0{,}5\left(\frac{x}{t} - \frac{a}{t}\right)\left(1 - \frac{x}{t} + \frac{a}{t}\right) + 0{,}5\left(\frac{a}{t}\right)\left(0{,}5 - \frac{x}{t} + \frac{2}{3}\frac{a}{t}\right) + 0{,}5\ \omega_f \frac{\varepsilon_{mu}}{\varepsilon_{fe}} \frac{\left(1 - \frac{x}{t}\right)}{\left(\frac{x}{t}\right)} \qquad (16)$$

$$\text{con } \left(\frac{a}{t}\right) = \frac{\varepsilon_{me}}{\varepsilon_{mu}}\left(\frac{x}{t}\right) \qquad (17)$$

AXIAL LOAD-MOMENT INTERACTION DIAGRAMS

Three FRP systems have been chosen, although they cannot be representative of the whole market products, they present properties compatible with current commercial products and are illustrative of formats that are used recurrently in practical applications and research tests.

- An unidirectional glass fiber sheet with $E_f\ t_f$ equal to 25 000 N/mm and ε_{fu}^* equal to 0.020.
- An unidirectional carbon fiber sheet with $E_f\ t_f$ equal to 40 000 N/mm and ε_{fu}^* equal to 0.016.
- A pultruded carbon strips with $E_f\ t_f$ equal to 200 000 N/mm and ε_{fu}^* equal to 0.017.

As stated above, the FRP design strain (ε_{fe}) are obtained by means of some factors to take into account the effects of long-term exposure to different environments ("*environment reduction factor*" or C_E) or FRP debonding induced by intermediate cracks ("*bond reduction factor*" or K). It was proposed a K factor equal to 0.40 for FRP wet lay-up systems and 0.25 for CFRP pultruded laminates and the C_E factor can be taken from ACI codes.

Table 1 shows the range of values of FRP design strain (ε_{fe}) for internal and external exposure (not aggressive environments) and the three FRP systems. As it can be seen, the values of ε_{fe} are between 0.006 and 0.0035.

Table 1. FRP design strain for different FRP systems

Exposure	**FRP system**	**$E_f\ t_f$**	**ε_{fu}***	**C_E**	**K**	**ε_{fe}**
Internal	GFRP unidirectional sheets	25 000	0.020	0.75	0.40	0.0060
	CFRP unidirectional sheets	40 000	0.016	0.95	0.40	0.0061
	Pultruded CFRP strips	200 000	0.017	0.95	0.25	0.0040
External	GFRP unidirectional sheets	25 000	0.020	0.65	0.40	0.0052
	CFRP unidirectional sheets	40 000	0.016	0.85	0.40	0.0054
	Pultruded CFRP strips	200 000	0.017	0.85	0.25	0.0036

Axial load-moment diagrams

Using the before calculating procedure, interaction diagrams are prepared. Figure 4 and 5 show non-dimensional axial load-moment diagrams for FRP design strain (ε_{fe}) equal to 0.0035 and 0.006, respectively. Besides, Figure 6 shows axial load-moment diagram for a higher value of FRP design strain (ε_{fe}), equal to 0.012, taking into account some theoretical situations in which bond requirements would be less demanding, for instance, retrofitting systems that covers full masonry surface (even TMR systems).

In these graphics, the axial load-moment curve for the unstrengthened wall section is drawn with broken line and the curves for different mechanical FRP reinforcement ratios (ω_f) are drawn with continuous line. The domains or regions (see Figure 3) related to the different failure modes are also indicated (AI and AII region are associated to FRP failure and B region to masonry crushing).

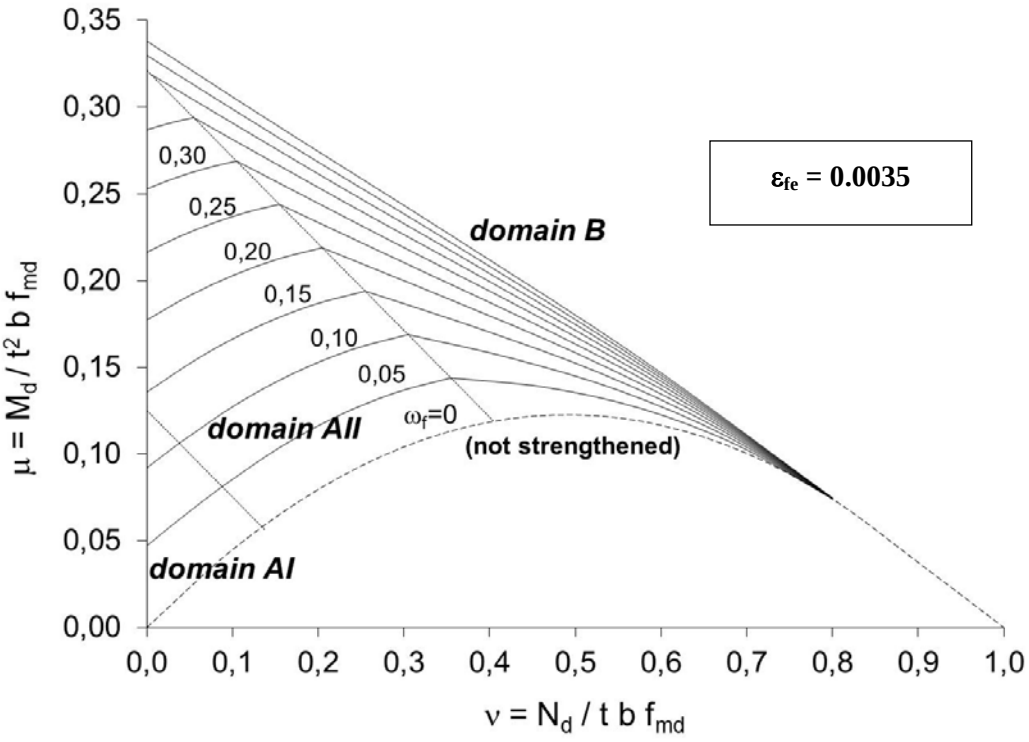

Figure 4: Non-dimensional axial load-moment diagram for ε_{fe}=0.0035

Figure 4: Non-dimensional axial load-moment diagram for ε_{fe}=0.0035

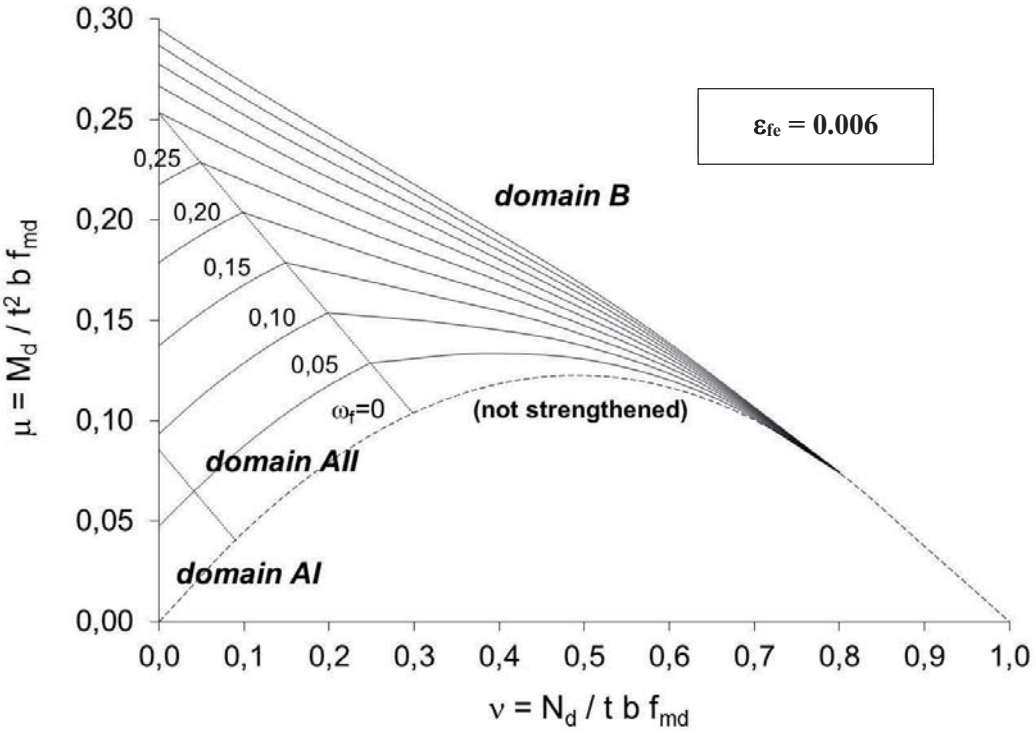

Figure 5: Non-dimensional axial load-moment diagram for ε_{fe}=0.006

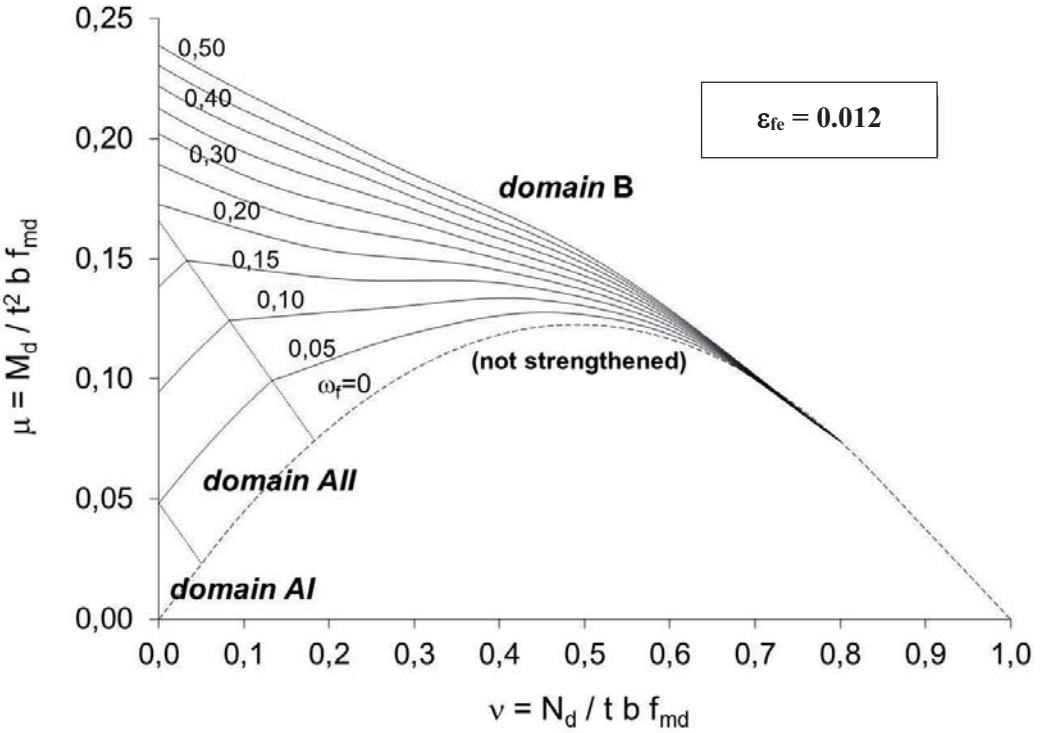

Figure 6: Non-dimensional axial load-moment diagram for ε_{fe}=0.012

These interaction diagrams allow to assess the predictable failure mode (due to masonry or FRP) and the improvement of the out-of-plane flexural sectional cross capacity depending on axial load level supported by the wall. Besides, they can be used to study the incidence of different parameters.

ANALYSIS OF THE DIAGRAMS

Comparing the previous diagrams, it can be observed that AI and AII regions (related to a predictable failure mode due to FRP) are more extensive for the lower value of FRP design strain (ε_{fe} equal to 0.0035). On the other hand, region B (masonry crushing) is prevailing for the higher value of FRP design strain (ε_{fe} equal to 0.012).
It may be highlighted that in region AI and AII the curves are almost parallel. This means that for a similar increase of mechanical amount of FRP ratio (ω_f) we can get a similar bending capacity improvement. However, in region B (masonry compression failure), the obtained moment enhancement by increasing the amount of reinforcement is smaller for larger reinforcement ratios and this increase is only possible when axial loads aren't great. The curves are practically overlapped for a normalized axial load (ν) equal to 0.7-0.8.
Figure 7 shows one of the interaction diagrams above (ε_{fe}=0.006) in more detail to distinguish the degree of flexural capacity improvement obtained with the reinforcement depending on the domain was A or B.

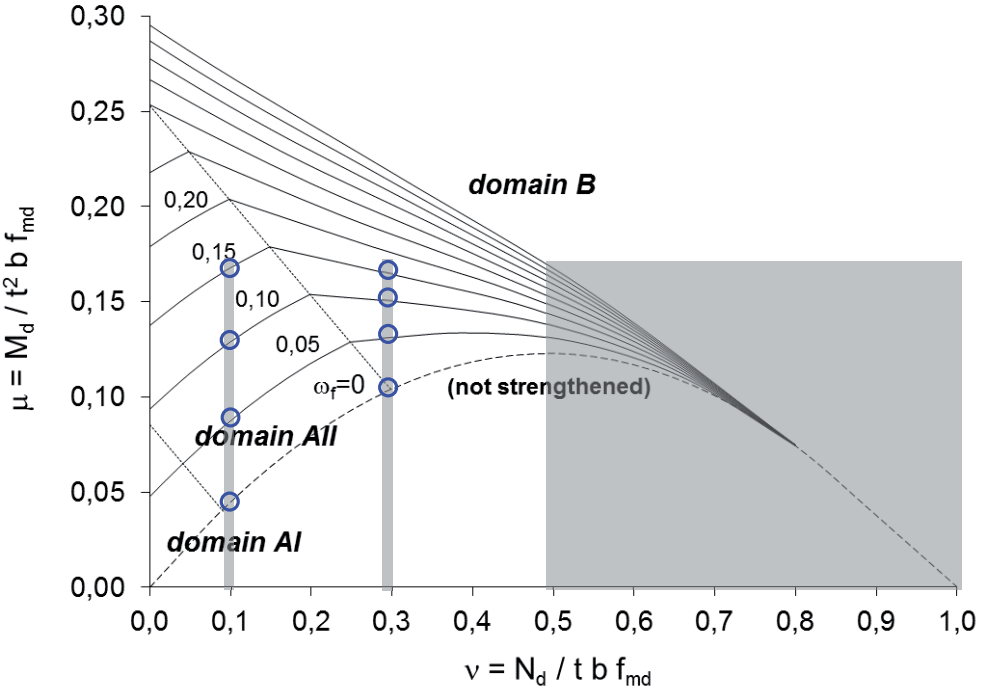

Figure 7: Different degree of out-of-plane flexural improvement depending on axil load level (ε_{fe}=0.006)

PARAMETER: AXIAL LOAD

Axial load level supported by the strengthened wall is the key factor and affects the predictable failure mode, the improvement of the bending capacity achieved with the reinforcement and, even, the viability, or not, of the strengthening intervention itself.
As we can see from diagrams, masonry crushing is usually expected failure for strengthened walls with moderate and high axial loads and/or with significant mechanical FRP reinforcement ratios (ω_f).
Regarding to the degree of out-of-plane flexural improvement achieved thanks to FRP strengthening, the enhancement is important for low axial load levels, in fact, great gains are obtained in experimental tests when strengthened samples are tested on pure bending. For instance, as we can see in Figure 7, for a normalized axial load (ν) equal to 0.10, the bending capacity of strengthened section is higher than 2.5 the unstrengthened one if ω_f is equal to 0.10 (equivalent to a masonry wall with f_{md} equal to 2.5 N/mm^2, one and a half feet of thickness, with FRP sheets with E_f t_f equal to 40 000 N/mm^2 over 30% of the masonry surface).
However, for a normalized axial load (ν) equal to 50% (Fig. 7), the increase of bending moment obtained with the reinforcement decreases considerably, regardless the amount of glued FRP. For ν equal to 70-80%, the improvement is negligible, this happens for all the different FRP systems analyzed (Fig.4-6).
In general, up to the half of the ultimate axial load on pure compression, the problem of the design of a masonry wall is fundamentally to guarantee its stability. It is in this range of axial loads where the strengthening intervention makes sense. In contrast, for high axial load levels the problem is related to the compressive strength, so adding a

material that is capable of withstanding large tensile forces but not compressions, hardly implies improvement and the strengthening operation has no sense. For this reason, it is important, previous of any intervention, to assess the actual load situation of the masonry element.

PARAMETER: FRP DESIGN STRAIN

The value used as FRP design strain has also impact on the type of predicted failure mode and on the assessment of ultimate bending capacity of the section.

Figure 8 shows the interaction diagram for a strengthened masonry section calculated with two values of FRP design strain (ε_{fe}), equal to 0.005 (black line) and 0.016 (red line), and their comparative with the unstrengthened section (broken line). In this figure, it has been drawn the curve for a masonry wall with thickness equal to one and a half feet, strengthened with a FRP sheets with $E_f\, t_f$ equal to 40 000 N/mm^2 over 30% of masonry surface.

As it can be seen, the value of FRP design strain (ε_{fe}) influences the type of predicted failure: high values of FRP design strain (ε_{fe} equal to 0.016) leads to predict failure mode due to the masonry and overestimate the ultimate bending moment. Only in the case that the deformation domain of the section at failure was type B, ε_{fe} doesn´t affect the prediction of the moment. The problem is, excepting extreme cases, the value of ε_{fe} must be previously established to predict which deformation domain of the section would be at failure.

In any case, using for calculation a low value of FRP design strain (ε_{fe}) is a safety practice. With this reduced value, we obtain smaller values (if the critical section is in domain AII) or equals (if it is in domain B) of the predictable ultimate bending capacity.

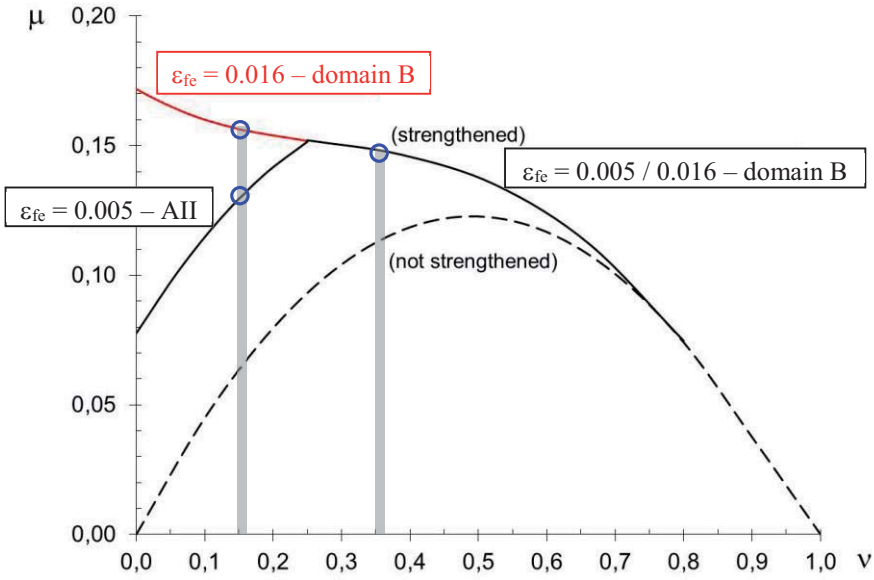

Figure 8: Different degree of out-of-plane flexural improvement depending on axil load level

CONCLUSIONS

Non-dimensional axial load-moment interaction diagrams which are suitable for different FRP systems have been prepared with the aid of an U.L.S. method for masonry wall sections with external FRP strengthening subject to bending and compression. These interaction diagrams are a useful tool for design and check FRP strengthened masonry walls, but also let analyzing the incidence of different parameters, such as axial load level, on the out-of-plane bending capacity of strengthened sections. It can be concluded:

Axial load level supported by the reinforced wall is the key factor and affects the predictable failure mode, the improvement of the bending capacity achieved with the reinforcement and, even, the viability, or not, of the strengthening intervention itself.

For low or moderate axial load level (normalized axial load “ν” lower than 50%), gluing FRP strengthening to masonry wall surface can lead to important improvement of out-of-plane flexural capacity. However, if the masonry wall supports high compressive loads, FRP strengthening operation has no sense. Previous of any intervention, it is important to assess the actual load situation of the masonry element.

Using for calculation a low value of FRP design strain (ε_{fe}) is a safety practice. With this reduced value, we obtain smaller values (if the strain distribution of the section is in domain AII) or equals (if it is in domain B) of the predictable ultimate bending capacity.
For low or moderate axial load levels, increase the FRP reinforcement rate (ω_f) means higher bending capacity. However, as stated above, for high axial load level (axial load over 70%-80% of the ultimate load in pure compression), increasing the amount or elastic modulus of FRP does not mean significant moment improvements.

ACKNOWLEDGE

This work is part of the Project PIE 201760E066 "*Experimental Analysis and Assessment of Structural Systems*" funded by the Spanish National Research Council and the Project BIA 2016-80310-P "*Study on FRP strengthening of rectangular reinforced concrete columns based on full-scale tests and proposal of a new design model*" funded by AECI and FEDER.

REFERENCES

Accardi M.; Cucchiara C., Faila A., La Mendola L. (2007). "CFRP flexural strengthening of masonry walls: experimental and analytical approach", Proceedings of FRPRCS-8 Conference, University of Patras, Greece.

Albert M. L., Cheng R.J.J., Elwi E. E. (1998). "Rehabilitation of Unreinforced Masonry Walls with Externally applied Fiber Reinforced Polymers", Structural Engineering Report nº 226, University of Alberta, Department of Civil & Environmental Engineering.

Barbieri A. (2000), "Interventi Strutturali su Edifici Storici in Muratura: Elementi Pressoinflessi, Rinforzati con Materiale Composito", PhD Thesis, University of Lecce.

Celestini G., Casadei P. (2009). "Innovation on Advanced Composite Materials for Strengthening and Protection of Historical Masonry Structures", Proceedings of "Meccanica delle strutture in muratura rinforzate con compositi: modellazione, sperimentazione, progetto, controllo", Venezia, Edición de C. Gentilini.

Di Tommaso A., Focacci F. (2001). "Strengthening Historical Monuments with FRP: a Desgin Criterial Review". Proceedings of "Composites in Construction: A Reality", edited by E. Cosenza, G. Manfredi, A. Nanni, pp. 223-230.

Galati N., Tumialan G., Nanni A. (2003). "Arching Effect in Masonry Walls Reinforced with Fiber Reinforced Polymer (FRP) Materials", Structural Report CIES 03-33, Center for Infrastructure Engineering Studies (CIES), University of Missouri-Rolla.

Hamilton III H. R. And Dolan C. W. (2001). "Flexural Capacity of Glass FRP Strengthened Concrete Masonry Walls", Journal of Composites for Construction, v. 5, nº 3, pp. 170-178.

Hendry A. W. 1998. "Structural Masonry. Second Edition", Macmillan Press LTD.

Martínez S. (2013). "Comportamiento estructural de elementos de fábrica reforzados con materiales compuestos avanzados solicitados a flexión y flexocompresión", PhD Thesis, Escuela Técnica Superior de Arquitectura de Madrid (UPM).

Martínez S., Gutiérrez J. P., García M. D. (2014). "Model Proposal for Flexural FRP Strengthening of Masonry Walls", IABSE Symposium Report, v.102, nº 30, pp. 874-879.

Morbin A. (2002). "Strengthening Masonry Elements with FRP Composites", Structural Report CIES 02-23, Center for Infrastructure Engineering Studies (CIES), University of Missouri-Rolla.

Mosallam A. S. (2007), "Out-of-plane Flexural Behavior of Unreinforced Red Brick Walls Strengthened with FRP Composites", Composites. Part B: Engineering, v. 38, nº 5, pp. 559-574.

Tan K. H., Patoary M. H. (2004). "Strengthening of Masonry Walls Against Out-of-plane Loads Using Fiber-Reinforced Polymer Reinforcement", Journal of Composites for Construction, v. 8, nº 1, pp: 79-87.

Triantafillou T. C. (1998). "Strengthening of Masonry Using Epoxy-Bonded FRP Laminates", Journal of Composites for Construction, v. 2, nº 2, pp: 96-104.

Velázquez-Dimas J. I., Ehsani M.R. (2000). "Modeling Out-of-plane Behavior of URM Walls Retrofitted with Fiber Composites", Journal of Composites for Construction, Vol. 4, No. 4, pp: 172-181.